

# An ultra-fast C-NOT gate based on electric dipole coupling between nitrogen-vacancy color centers

SHI Shunyang<sup>1,2,3,4</sup>, JI Wentao<sup>1,2,3,4</sup>, WANG Ya<sup>1,2,3,4\*</sup>, DU Jiangfeng<sup>1,2,3,4\*</sup>

1. Department of Modern Physics, University of Science and Technology of China, Hefei 230026, China;

2. Hefei National Laboratory for Physical Sciences at the Microscale, Hefei 230026, China;

3. CAS Key Laboratory of Microscale Magnetic Resonance, University of Science and Technology of China, Hefei 230026, China;

4. Synergetic Innovation Center of Quantum Information and Quantum Physics, University of Science and Technology of China, Hefei 230026, China

\* Corresponding author. E-mail: ywustc@ustc.edu.cn; djf@ustc.edu.cn

**Abstract:** Our research proposes a new scheme to build a controlled-NOT (C-NOT) gate between two adjacent nitrogen-vacancy (NV) color centers in diamond, using electric dipole coupling between adjacent NVs and selective resonant laser excitation. The electric dipole coupling between two NVs causes the state dependent energy shift. This allows to apply resonant laser excitation to realize the C-phase gate. Combined with a single qubit operation, C-NOT gate can be implemented quickly. Between two adjacent 10 nm NVs, the C-NOT gate can operate up to 120 ns faster than the traditional magnetic dipole coupling method by 2 magnitudes. In order to reduce the effect of a spontaneous emission, we propose to use a non-resonant cavity to suppress the spontaneous emission. The simulation results show that the C-phase gate fidelity can reach 98.88%. Finally, the scheme is extended to a one-dimensional NV spin chain.

**Keywords:** nitrogen-vacancy color center; quantum computing; C-NOT gate; 1D-spin chain

**CLC number:** O413      **Document code:** A

## 1 Introduction

Because of the great prospect of the quantum computing and quantum communication, there has always been a desire to implement a scalable, fault-tolerant, coherent, fully controlled quantum system in a physical system<sup>[1]</sup>. Ion traps, superconducting circuits, quantum dots, and solid-state spins are all strong competitors to achieve this goal. The NV color center in diamond, which has the advantages of a long coherence time<sup>[2]</sup>, optical initialization and reading<sup>[3]</sup>, has been the focus of research for a long time, such as the manipulation of NV color center electrons<sup>[4]</sup>, entanglement of electrons with nuclear spin, magnetic detection<sup>[5]</sup>. Using the hyperfine coupling between NV and a nuclear spin, combined with frequency-selecting microwave and radio frequency pulses, C-NOT operation between the NV electron spin and adjacent nuclear spin has been realized<sup>[6]</sup>. The long coherence time indicates that there is more time available to perform the quantum operation before the system is decoherent. But it also desires the fast operation, otherwise the advantage of the long coherence time will be offset. So, a fast gate operation scheme is required, and the rapid implementation of the two qubit C-NOT gate is the key in all schemes.

The most used manipulation of the NV color center is to perform single qubit operations via the interaction of the microwave with the magnetic dipole<sup>[7-8]</sup>. In order to shorten the operating time, the optical holonomic single-qubit gate was proposed<sup>[9]</sup>. Using the geometric interference of polarized light and NV's spin-orbit interaction, the full control of NV spin-1 subspace has been realized<sup>[9]</sup>. However, this is limited to a single NV. As for two qubit operation of two NVs, via bell-state measurement of the two NV's zero phonon line (ZPL) photons, entanglement is generated between the two NVs over a long distance<sup>[10]</sup>. But the whole process is inefficient, complex, difficult and not fully coherent. This research extends the optical quantum control from a single-qubit to two qubits, and proposes a scheme that can do C-NOT operation rapidly and efficiently between two adjacent NVs.

The core of the C-NOT gate is a C-phase gate. That is to selectively provide  $\pi$  phase (i. e., multiply  $-1$ ) for one of the 4 base states ( $|00\rangle$ ,  $|01\rangle$ ,  $|10\rangle$ ,  $|11\rangle$ ) of two qubits. The Rabi oscillation between the state and an auxiliary excited state under resonant laser excitation goes through a  $2\pi$  cycle, which exactly provides  $\pi$  phase for the state. Here we use electric

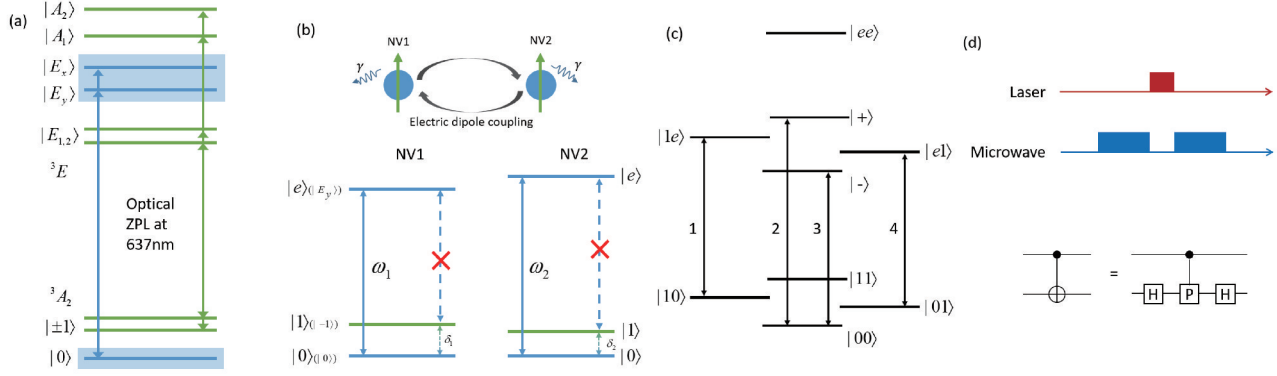


**Figure 1.** (a) NV color center energy level structure and transition properties. (b) Each NV can be simplified into a three-level system. There is a transition channel between  $|0\rangle$  and  $|e\rangle$ , and transition between  $|1\rangle$  and  $|e\rangle$  is forbidden. (c) The  $|+\rangle$  and  $|-\rangle$  in the figure respectively represent the high and low energy state of mixed states between  $|0e\rangle$  and  $|e0\rangle$ . There are four transition channels with different frequencies. (d) The pulse sequence forming the C-NOT gate: two hadamard gates combined with a C-phase gate.

dipole coupling between NVs to remove degeneracy and create a difference in excitation frequency to ensure that only one ground state will be excited and thus experiences a  $2\pi$  Rabi oscillations. Similar methods have precedents in the Rydberg atom system<sup>[11–13]</sup>. The electric dipole coupling is also used to implement a C-phase gate in the Rydberg atom system, such as the dipole blockade of excitation<sup>[13–14]</sup>.

Spontaneous radiation originates from the interaction between NV's electric dipole moment and a vacuum fluctuating field. It is not difficult to imagine that there is an electric dipole coupling between two adjacent NVs, like a common magnetic dipole coupling. As long as the distance between two NVs is small enough, the electric dipole coupling is strong enough. The coupling will cause the state mixing and energy level shift, especially the energy level shift is related to their spin state. So if the coupling is strong enough that transitions are no longer degenerate, a resonant laser excitation can be used to excite a specific transition which allows us to build an ultra-fast C-NOT gate.

This paper studies and proposes a new C-NOT gate scheme based on the electric dipole coupling between NVs at low temperatures. It can perform C-NOT operation on two adjacent NVs through microwaves and laser pulses. The operation is extremely fast, which shows that the same coherence time allows the construction of a quantum circuit with greater depth. Secondly, we numerically studied the effectiveness and fidelity of the scheme. Through the analysis of the parameters, an auxiliary method is proposed to improve the fidelity, which is to put the NV color center into the non-resonant optical cavity to suppress the spontaneous radiation. At last, the scheme is extended to a one-dimensional NV spin chain. We believe that this research will lay the foundation for the scalability and

complete the control of the NV system.

## 2 Basic theory

According to the optical transition characteristics of the NV color center, transitions are allowed between the excited state  $|E_x\rangle$ ,  $|E_y\rangle$  and the ground state  $|m_s=0\rangle$ . Transitions are also allowed between the excited state  $|E_1\rangle$ ,  $|E_2\rangle$ ,  $|A_1\rangle$ ,  $|A_2\rangle$  and the ground state  $|m_s=\pm 1\rangle$ , and the rest are forbidden<sup>[15]</sup> (Figure 1 (a)). First, we use two NV color centers that are very close (about 10 nm), and use their respective  $|E_y\rangle$ ,  $|m_s=0\rangle$  (logical 0),  $|m_s=-1\rangle$  (logical 1) to construct a C-NOT gate. Each NV color center can be regarded as a three-level system (Figure 1 (b)). We use  $|e\rangle$  to represent  $|E_y\rangle$ ,  $|0\rangle$  to represent  $|m_s=0\rangle$ , and  $|1\rangle$  to represent  $|m_s=-1\rangle$ . The solid arrow represents the allowed optical transition. It can be seen that transitions between  $|0\rangle$  and  $|e\rangle$  are allowed, and transitions between  $|1\rangle$  and  $|e\rangle$  are prohibited. This means that the electric dipole operator  $\mathbf{d}$  expands under the base vector:  $\langle e|\mathbf{d}|0\rangle \neq 0$  and  $\langle e|\mathbf{d}|1\rangle = 0$ .

On this basis, the electric dipole coupling term in the Hamiltonian is<sup>[16–17]</sup>

$$H_{dd} = \frac{1}{4\pi\epsilon_0} \frac{1}{|\mathbf{r}_{12}|^3} [\mathbf{d}_1 \cdot \mathbf{d}_2 - 3(\mathbf{d}_1 \cdot \hat{\mathbf{r}})(\mathbf{d}_2 \cdot \hat{\mathbf{r}})] \quad (1)$$

$\mathbf{d}_1$  and  $\mathbf{d}_2$  are the electric dipole operators of NV<sub>1</sub> and NV<sub>2</sub> respectively.  $\mathbf{r}_{12}$  is the relative position vector between NV<sub>1</sub> and NV<sub>2</sub>.  $\hat{\mathbf{r}} = \mathbf{r}_{12}/|\mathbf{r}_{12}|$ , is the unit vector in the direction of  $\mathbf{r}_{12}$ .  $\epsilon_0$  is the vacuum dielectric constant. Since the diagonal element of the NV's electric dipole is almost zero<sup>[18]</sup>, the non-diagonal element only has a non-zero value between  $|e\rangle$  and  $|0\rangle$ . The electric dipole can be expanded into an operator form:

$$H_{dd} = \hbar\nu(|00\rangle\langle ee| + |ee\rangle\langle 00| + |0e\rangle\langle e0| + |e0\rangle\langle 0e|) \quad (2)$$

Here assume that  $d_1 = \langle e | \mathbf{d}_1 | 0 \rangle$  and  $d_2 = \langle e | \mathbf{d}_2 | 0 \rangle$  are real. This form indicates that energy level shift and state mixing only occur in the states related to  $|e\rangle$  and  $|0\rangle$ , but it does not affect the rest of the states. In Eq. (2),

$$\hbar\nu = \frac{1}{4\pi\epsilon_0} \frac{1}{|\mathbf{r}_{12}|^3} [d_1 \cdot d_2 - 3(d_1 \cdot \hat{\mathbf{r}})(d_2 \cdot \hat{\mathbf{r}})] \quad (3)$$

Using the relationship between a spontaneous emission and a transition electric dipole, it can be estimated that when two NV color centers are separated by about 10 nm,  $\nu = 2\pi \times 414$  MHz. The Hamiltonian of the two NVs themselves is

$$H_0 = H_{\text{NV1}} + H_{\text{NV2}} = \hbar\omega_1 |e\rangle_1 \langle e| + \hbar\delta_1 |1\rangle_1 \langle 1| + \hbar\omega_2 |e\rangle_2 \langle e| + \hbar\delta_2 |1\rangle_2 \langle 1| \quad (4)$$

The ground state  $|0\rangle$  and  $|1\rangle$  have an interval of 2.87 GHz due to the zero-field splitting, and can be adjusted by a magnetic field, which are represented by  $\delta_1$  and  $\delta_2$ . The angular frequency of the transition between  $|0\rangle$  and  $|e\rangle$  can be adjusted by stress<sup>[19]</sup> or the electric field<sup>[20]</sup>, denoted by  $\omega_1$  and  $\omega_2$  respectively.

The overall Hamiltonian with no external field applied is

$$H_{\text{total}} = H_0 + H_{dd} \quad (5)$$

Since the  $H_{dd}$  contributes non-diagonal items  $|00\rangle\langle ee|$  and  $|0e\rangle\langle e0|$ , the linear superposition states of  $|00\rangle$  and  $|ee\rangle$ , and the linear superposition states of  $|0e\rangle$  and  $|e0\rangle$  form new four eigenstates. The resulting energy level diagram is shown in Figure 1(c). Due to the large energy gap, the state mixing between  $|00\rangle$  and  $|ee\rangle$  can be safely ignored and  $E_{|00\rangle} \approx 0$ ,  $E_{|ee\rangle} \approx \omega_1 + \omega_2$ . After calculation:

$$E_{\pm} = \frac{(\omega_1 + \omega_2) \pm \sqrt{\alpha^2 + 4\nu^2}}{2} \quad (6)$$

where  $\alpha = \omega_2 - \omega_1$ . It can be seen that the role of the electric dipole coupling  $\nu$  is to make the energy levels more separated from each other. The arrow in Figure 1(c) indicates there are 4 allowed transitions.

Based on this new energy level structure, the resonant excitation is explored to realize the desired fast C-phase gate. The key idea is to achieve a  $2\pi$  optical gate of one specific transition while leaving the other transitions unaffected. For example, A  $2\pi$  optical Rabi oscillation between  $|01\rangle$  and  $|e1\rangle$ , will make  $|01\rangle$  become  $-|01\rangle$  and the other three states unchanged. This ultra-fast C-phase gate, can be combined with a microwave single-qubit operation to form a C-NOT gate (Figure 1(d)). The laser drive Hamiltonian is

$$H_{\text{drive}} = -\mathbf{d} \cdot \mathbf{E} = \frac{1}{2} \hbar g_1 (e^{i\omega t} + e^{-i\omega t}) (|0\rangle_1 \langle e| + |e\rangle_1 \langle 0|) + \frac{1}{2} \hbar g_2 (e^{i\omega t} + e^{-i\omega t}) (|0\rangle_2 \langle e| + |e\rangle_2 \langle 0|) \quad (7)$$

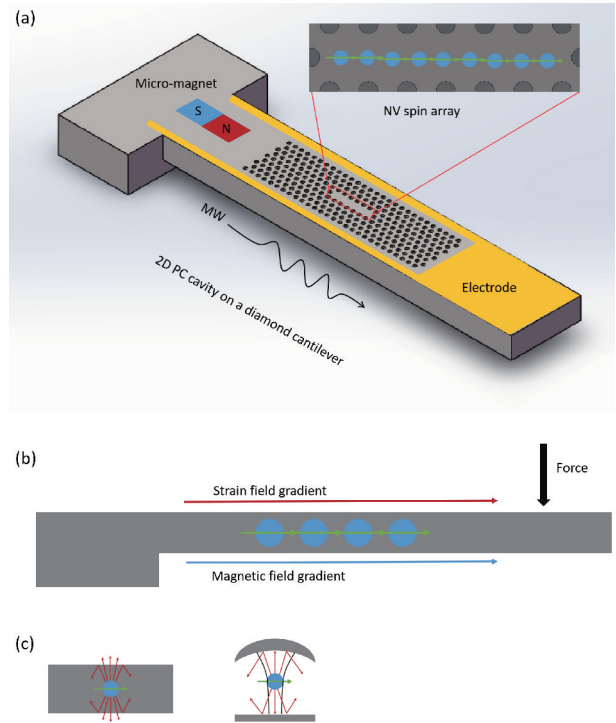


**Figure 2.** (a) Experimental conception: A two-dimensional photonic crystal cavity is machined on the diamond cantilever, and the NV array is placed in it. Metal electrodes are attached to the top of the beam, and the stress can be controlled by an external electric field. The magnet provides a gradient magnetic field. The cantilever will be placed in a radiating structure to receive microwave pulses. (b) Magnetic field gradient and stress gradient. (c) The schematic diagram of the photonic crystal cavity (left) and the Fabry-Perot cavity (right) respectively. For a dipole radiation source in a cavity, the photonic crystal cavity can confine most of the radiation, while the Fabry-Perot cavity allows most of the radiation to escape.

$\omega$  is the laser angular frequency, here let  $\omega = \omega_1$  and consider that  $g_1 = g_2 = g$ . Here the transition 4 is taken as an example to show the fast C-phase operation. When the coupling strength is  $g/2\pi \approx 50$  MHz, the C-phase operation takes 20 ns. Compared with the scheme using the magnetic dipole coupling between NVs (coupling strength is about 100 kHz when the interval is 8 nm), whose phase accumulation takes about 10  $\mu$ s to realize the C-phase gate<sup>[21]</sup>, operation speed of our scheme is two orders of magnitude faster.

The simultaneously hadamard gate need to be executed with suitable microwave pulses. The ground state energy level interval of the NV color center can be adjusted by a gradient magnetic field. Microwave pulse can implement a single-qubit operation with fidelity greater than 0.99<sup>[7,8]</sup>. In such schemes dynamically corrected gates (DCGs)<sup>[4]</sup> can be combined to further suppress the dominant dephasing process. For a typical dephasing time ( $T_2^*$ ) with a few microseconds to a

dozen microseconds<sup>[22]</sup>. The DCGs<sup>[4]</sup> can extend the coherence time by two orders of magnitude, reaching 600  $\mu\text{s}$ , which is close to the  $T_1$  relaxation limit of the NV color center. The cost is only a tenfold increase in the duration of the pulse operation.

The required individual control of each NV center can be realized by applying a gradient magnetic field. For a reported magnetic gradient of  $1 \text{ MT} \cdot \text{m}^{-1}$ <sup>[23]</sup>, 10 nm separation between two NVs have a magnetic field difference of 100 Gs, corresponding to a frequency difference of 280 MHz. This means a Hardmard gate can be implemented in about 50 ns. The execution time of the entire C-NOT gate is about 120 ns (about 10  $\mu\text{s}$  in the traditional scheme). The execution time is 2 orders of magnitude smaller than the coherence time.

### 3 Parametric analysis

In this part, the factors affecting the fidelity of the operation is analysed. First, it is necessary to ensure that the resonance laser only excites the Rabi oscillation of the transition 4, and leave the transitions 1, 2, 3 unaffected. This requires the transition 4 to be separated in frequency from others, that is

$$\Delta_{4,1} \gg g, \Delta_{4,3} \gg g \quad (8)$$

$g$  is the coupling strength between the light field and the NV color center.  $\Delta_{4,1}$ ,  $\Delta_{4,3}$  represents the absolute value of the frequency difference between transition 4 and transition 1, 3. For the former case, the stress or electric field can be used. For the latter case, the electric dipole coupling  $\nu$  should be as large as possible, and  $\Delta_{4,1} = \alpha$  should not be too large. Note that:

$$\Delta_{4,3} = (\sqrt{\alpha^2 + 4\nu^2} - \alpha)/2 \quad (9)$$

We choose  $\alpha = \nu/\sqrt{2}$ , so that  $\Delta_{4,3} = \Delta_{4,1} = \nu/\sqrt{2}$ . Second, we hope that the transition peak is as narrow as possible. Since the spontaneous radiation  $\gamma$  (NV lifetime is 12 ns<sup>[24]</sup>) will impair the fidelity of optical Rabi, so this requires that

$$g \gg \gamma \quad (10)$$

The larger the  $g$ , the smaller the C-phase gate operation time  $2\pi/g$ . Combining the above two points, it can be found that the coupling intensity  $g$  cannot be too large or too small. The spontaneous radiation rate  $\gamma$  sets a lower limit, and the interval between transition peaks  $\Delta_{4,3}$ ,  $\Delta_{4,1}$  sets an upper limit.

To reduce the lower limit, here we explore the Purcell effect of optical cavity. Many experiments have used cavities to control the spontaneous emission, such as using superconducting microwave cavities to increase the relaxation rate of solid spins<sup>[25]</sup>, enhancing the spontaneous emission of Rydberg atoms<sup>[26]</sup>. The optical cavity can be used to enhance the spontaneous radiation at resonance<sup>[27,28]</sup>, and to suppress spontaneous radiation at non-resonance<sup>[29,30]</sup>. In fact, the excited state lifetime

of the NV color center in the nano-diamond can reach 21 ns<sup>[31]</sup>, which is longer than 12 ns in the bulk diamond, which shows that extending the lifetime is feasible.

According to the Purcell effect<sup>[32]</sup>, when the resonance wavelength of the optical cavity is equal to the zero phonon line (ZPL) of the NV color center, the ZPL of the NV color center will be enhanced. When the cavity resonance wavelength is shifted away from the optical resonance spectrum of NV, the spontaneous radiation will be suppressed. Regardless of enhancement or suppression, only part of radiation which enters the optical cavity in the correct direction can be affected. The electric dipole radiation occupies the azimuth angle of  $8\pi/3$  in the whole space. We hope that as much light energy enters the cavity as possible, and then be suppressed, so a 2D photonic crystal cavity is chosen (Figure 2 (a) (b)). The refractive index of the diamond is 2.42, and the probability that a spontaneous radiation escapes from the cavity without being bound by total reflection is  $P_{\text{leaky}} = 0.134$ . This means that under ideal conditions, all parts in the cavity can be suppressed and the spontaneous radiation rate is reduced to 0.134 times of the original. The lifetime can be extended to 7.5 times of the original. The 2D photonic crystal cavity has outstanding effect compared with other kinds of optical cavity, such as the Fabry-Perot cavity (FP cavity). The solid angle that can enter the cavity mode is extremely small, and a large amount of radiation directly escapes out of the cavity, and the suppression is almost negligible (Figure 2(c)).

### 4 Numerical simulation

The numerical simulation is used to verify the effectiveness of the entire scheme under the theory of part 2. The simulation ignores the imperfections of devices and microwave operations, and takes into account spontaneous emission, decoherence and unwanted non-resonant excitation, which are dominant error sources in the optical control. We first adopt ideal parameters, assuming that the extended lifetime of the NV color center is 60 ns, and the distance between two NVs is 5 nm, corresponding to  $\nu = 2\pi \times 3.312 \text{ GHz}$ . The result is shown in Figure 3(a). The process fidelity is around 98%, which proves that the experimental sequence does implement a C-NOT operation.

Secondly, we consider the effect of the optical control strength  $g$  by adjusting it in a range of  $\Delta_{4,1}, \Delta_{4,3} \gg g \gg \gamma$ . Since  $g$  only involves the C-phase step, only the fidelity of the C-phase gate is simulated. Set the initial state  $|\psi_0\rangle = 0.5(|01\rangle + |10\rangle + |00\rangle + |11\rangle)$ . The theoretical target state is  $|\psi_{\text{target}}\rangle = 0.5(-|01\rangle + |10\rangle + |00\rangle + |11\rangle)$ . The parameters and results are shown in



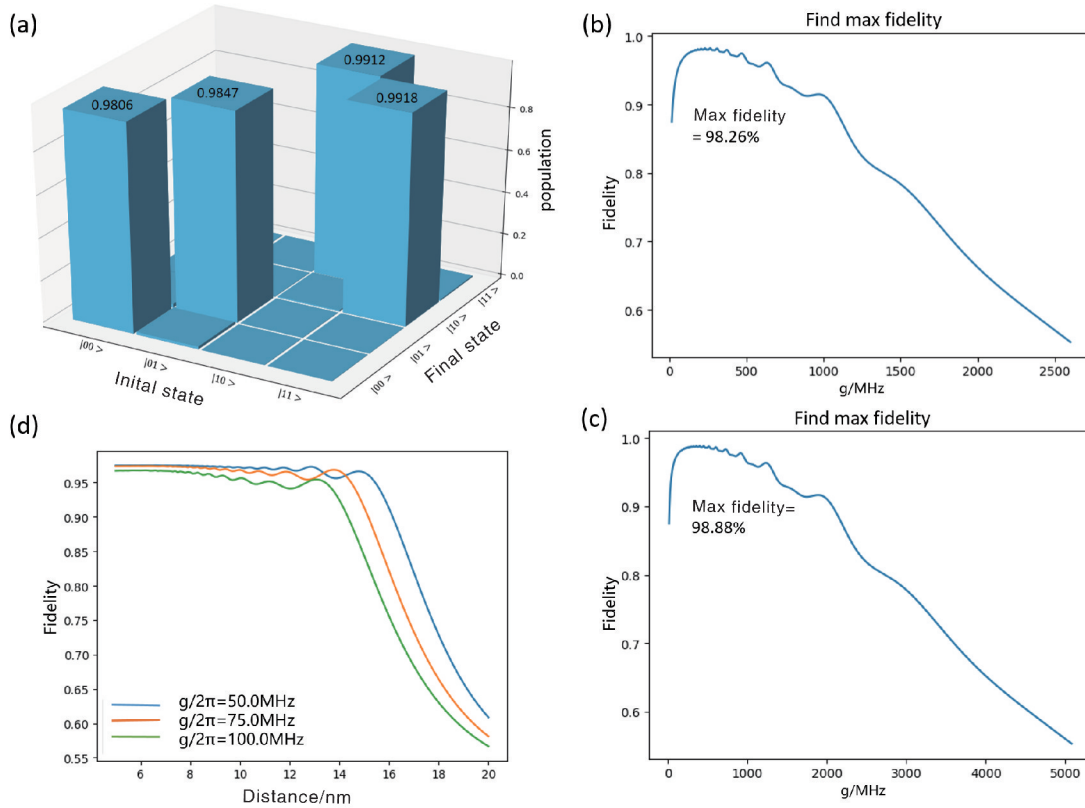


**Figure 3.** (a) The tomography simulation results of the C-NOT gate show that the probability distribution of the final state. It is obtained after the same pulse sequence in the four initial states respectively, which shows that the scheme indeed constitutes a C-NOT gate. (b), (c) With 10 nm and 8 nm interval respectively, the fidelity of the C-NOT changes with the coupling intensity  $g$ . (d) With three different coupling intensities, the simulated C-phase fidelity decreases as the distance increases.

Figures 3(b), 3(c). When the two NV color centers are separated by 10 nm and 8 nm, the maximum fidelity is 98.26% and 98.88% respectively. The smaller the distance, the stronger the electric dipole coupling. So with the weaker off-resonance excitation, higher fidelity can be reached. As  $g$  increases, the fidelity curve first rises rapidly and then falls. When  $g$  is too small, the spontaneous radiation will be dominant and reduces the fidelity. When  $g$  is too large, the laser will non-resonantly excite unwanted transitions 1, 2, 3. But the impair to fidelity is moderate. Further simulation shows that if the lifetime is prolonged 10 times (about 120 ns), the fidelity can reach 99.3% when the interval is 8 nm.

Finally, we consider the impact of the coupling strength  $\nu$  between two NVs. The parameters and results are shown in Figure 3(d). The coupling strength decreases with the inverse cubic of the distance. The increase of the interval  $|r_{12}|$  leads to the decrease of  $\nu$ , which in turn leads to the decrease of  $\Delta_{4,3}$ . In this situation the fidelity of the C-phase gate decreases due to the effect of the non-resonant excitation of other transitions. So the larger the optical control strength  $g$ , the faster the fidelity decreases. At the same time, the

simulation shows that as long as  $g$  is not particularly large, there is a slower-decreasing platform area before the rapid fall. When the interval is expanded from 5 nm to 15 nm, the fidelity is still higher than 95%.

## 5 Scalability

The aforementioned C-NOT gate scheme can be implemented in the case of 2 NVs. Naturally, it is desire to expand from 2 adjacent NV color centers to multiple NVs in a scalable way. Here we consider the C-NOT operation between any  $NV_i$  and  $NV_{i+1}$  in a one-dimensional NV spin chain. In this case, the electric dipole coupling between  $NV_{i+2}$  and  $NV_{i+1}$ ,  $NV_{i-1}$  and  $NV_i$  will affect the desired operation between  $NV_i$  and  $NV_{i+1}$ . For example, the C-NOT operation between  $NV_2$  and  $NV_3$  requires a resonant excitation of the transition between  $|01\rangle_{2,3}$  and  $|e1\rangle_{2,3}$ , however, the electric dipole coupling between  $NV_1$  and  $NV_2$ , will induce a  $NV_1$ 's state dependent frequency shift as shown in Figure 4(a). Undoubtedly this will greatly impair the fidelity.

To overcome this shortcoming, we consider a spin-chain configuration as shown in Figure 4(d). Some NV color centers are used as redundancy to shield the

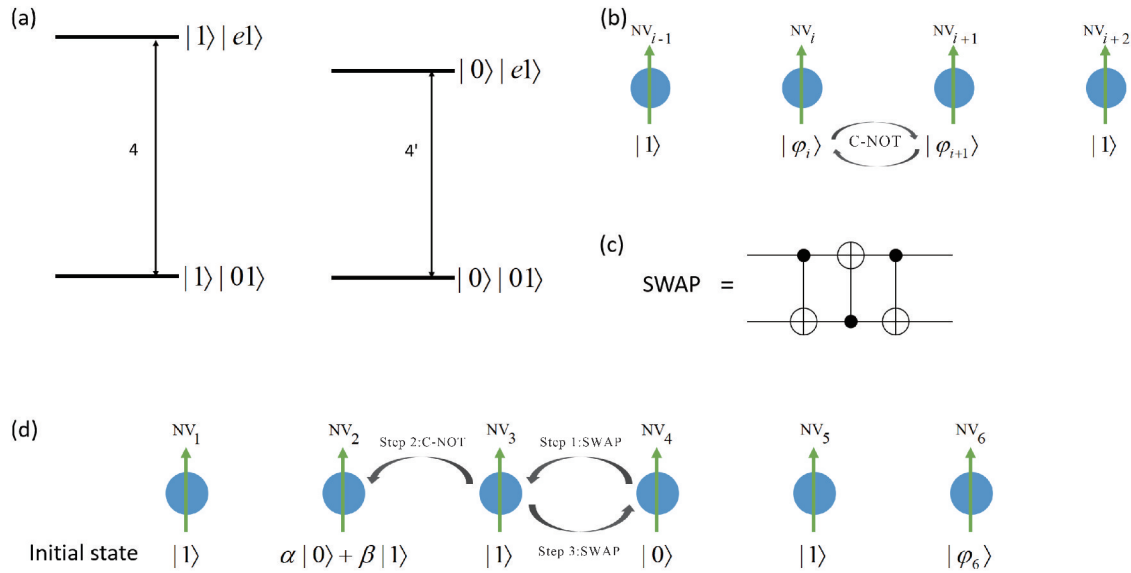


**Figure 4.** (a) The state of NV<sub>1</sub> will affect the transition frequency of NV<sub>2</sub> and NV<sub>3</sub>. (b) As long as one of NV<sub>i-1</sub> and NV<sub>i+2</sub> is in  $|1\rangle$ , C-NOT operation between NV<sub>i</sub> and NV<sub>i+1</sub> can be completed. (c) SWAP gate, consists of 3 C-NOT gate. (d) With redundant NV color centers, the SWAP-C-NOT-SWAP operation sequence can be used to implement a C-NOT operation and avoid the impair of additional electric dipole coupling.

unwanted electric dipole coupling (the second nearest neighbour coupling is ignored). Let the odd-numbered NV in the chain be the redundant auxiliary NV, all initialized to  $|1\rangle$ . And the even-numbered NV color center used for calculation, which can be in any state. We use NVs in  $|1\rangle$  as a shield because the energy shift only involves  $|0e\rangle$  and  $|e0\rangle$ . If C-NOT gate between NV<sub>i</sub> and NV<sub>i+1</sub> is being operated, at least one of NV<sub>i-1</sub> and NV<sub>i+2</sub> must be in  $|1\rangle$ , as shown in Figure 4(b). Due to symmetry, resonantly exciting transition 1 ( $\omega = \omega_2$ ) can also achieve the goal. So there are two C-NOT schemes between NV<sub>i</sub> and NV<sub>i+1</sub>, one is to resonantly excite NV<sub>i</sub>, the other is to resonantly excite NV<sub>i+1</sub> (with slightly different single-qubit operations). These two schemes can use either NV<sub>i</sub> or NV<sub>i+1</sub> as the control qubit. When NV<sub>i-1</sub> is in  $|1\rangle$ , C-NOT can be realized by exciting NV<sub>i</sub>. When NV<sub>i+2</sub> is in  $|1\rangle$ , C-NOT can be realized by exciting NV<sub>i+1</sub>. This enables us to do the SWAP gate.

In summary, the one-dimensional NV spin chain can be used as an extension scheme. For example, we want to operate C-NOT gates for NV<sub>2</sub> and NV<sub>4</sub>, shown in Figure 4(d). Suppose the initial state of NV<sub>2</sub> and NV<sub>4</sub> is  $|\phi_2\rangle = \alpha|0\rangle + \beta|1\rangle$ ,  $|\phi_4\rangle = |0\rangle$ . Step 1 is to exchange NV<sub>3</sub> and NV<sub>4</sub> with the SWAP gate, then  $|\phi_4\rangle = |1\rangle$ ,  $|\phi_3\rangle = |0\rangle$ . Step 2 is to perform C-NOT operations on NV<sub>2</sub> and NV<sub>3</sub>, after the operation  $|\phi_{2,3}\rangle = \alpha|00\rangle + \beta|11\rangle$ , NV<sub>2</sub> and NV<sub>3</sub> are entangled. Step 3 is to use the SWAP gate to exchange the states of NV<sub>3</sub> and NV<sub>4</sub>. After the exchange, NV<sub>2</sub> and NV<sub>4</sub> produce entanglement  $|\phi_{2,4}\rangle = \alpha|00\rangle + \beta|11\rangle$ . Note that in Steps

1 and 3, the SWAP gate is composed of 3 C-NOT gates<sup>[33]</sup>, as shown in Figure 4(c). Because NV<sub>5</sub> on the right side of NV<sub>4</sub> is on  $|1\rangle$  and the NV<sub>2</sub> on the left side of NV<sub>3</sub> is not in  $|1\rangle$ , so it is only feasible to implement these 3 C-NOT with a scheme to excite NV<sub>4</sub>.

This scheme introduces redundant qubits to avoid the influence of the adjacent electric dipole coupling, but also reduces the NV's utilization to half. At the same time, a C-NOT operation must be combined with two SWAP operations, which requires a total of 7 C-NOT. So it is best to use a large gradient magnetic field to implement rapid hard pulses.

The NV color center array separated by 1  $\mu\text{m}$  from each other<sup>[34]</sup> and silicon-vacancy color center separated by 500 nm<sup>[35]</sup> have been realized. The NV array with a spacing of 40 nm with a positioning accuracy of 10 nm has been realized<sup>[36]</sup>. Although it has not yet reached an array with an interval of 10 nm, with the advancement of micro-nano processing technology, we believe that this solution can be implemented in experiments in the future.

## 6 Conclusions

In summary, this study designed a C-NOT gate scheme based on the electric dipole coupling between adjacent NV color centers. The advantage is that the C-phase operation is very fast. Combined with a dynamically corrected gate (DCGs) that can greatly extend the coherence time and strong gradient magnetic fields, the execution time of C-NOT gates can be compressed to the order of hundreds of nanoseconds, which can be used to construct quantum circuits with depths of

thousands. And the fidelity of the C-phase gate can be improved by putting the NV color center into the non-resonant optical cavity. It is assumed that the lifetime can be extended by 5 times. Based on this, a series of numerical simulations verified the effectiveness of the entire pulse sequence, and calculated that the fidelity of the C-phase operation between two NV color centers with an interval of 8 nm can reach 98.88%. Then we simulated the trend of decreasing fidelity as the distance between two NVs increases. Finally, we exemplified how to extend the scheme to a one-dimensional NV spin chain. We believe that this kind of C-NOT gate based on the electric dipole coupling can be extended to other systems and has great potential for improvement, making this solution a cornerstone for quantum networks.

## Acknowledgments

This work is supported by National Key Research and Development Program of China (Nos. 2018YFA0306600, 2017YFA0305000), National Natural Science Foundation of China (Item Numbers: 11775209, 81788101, 11761131011), Anhui Quantum Information Technology Leading Project (Item Number: AHY050000), Fundamental Research Funds for the Central Universities and USTC Research Funds of the Double First-Class Initiative.

## Conflict of interest

The authors declare no conflict of interest.

## Author information

**SHI Shunyang** is currently a graduate student under the tutelage of Prof. Wang Ya at University of Science and Technology of China. His research interests focus on quantum information and quantum computation.

**WANG Ya** is a professor at University of Science and Technology of China (USTC). He received the PhD degree in science from USTC in 2012, and was awarded the 2012 Dean's Excellent Scholarship of the Chinese Academy of Sciences. From 2012 to 2016, he did post-doctoral research at University of Stuttgart, Germany. In 2016, he joined USTC. He mainly engaged in experimental research on solid-state quantum devices based on solid point defects and quantum computing applications. The main directions include 1) experimental research on the preparation of high-performance diamond quantum chips and quantum probes; 2) experimental research on spin-based quantum computing networks. Related research results were published in *Nature*, *Nature Photonics*, *Nature Nanotechnology*, *Nature Communications*, *Science advances*, *Physical Review Letters*, *Physical Review Applied*, *ACS Nano* and other academic journals, have been cited more than 1800 times (data from Google Scholar).

**DU Jiangfeng** (corresponding author) is an academician of the Chinese Academy of Sciences, a professor of the University of Science and Technology of China, a distinguished professor of the Yangtze River Scholars of the Ministry of Education, a winner of the National Science Fund for Outstanding Youth, a chief scientist

of a major national scientific research project, and a member of the first batch of National Ten Thousand Talents Program "Science and Technology Innovation Leaders", a national-level candidate for the New Century Talents Project. He mainly engaged in experimental research on quantum physics and its applications. He innovatively developed quantum physics experimental technologies such as spin quantum control and dynamics decoupling, combined with the successful development of a series of high-performance magnetic resonance experimental equipment, and improved the sensitivity and resolution of magnetic resonance detection to the international leading level. New applications of quantum physics such as quantum computing have achieved research results with important international influence. He has published more than 200 papers in international high-level academic journals including *Science*, *Nature*, *Physical Review Letter* and *Nature*-branded sister journals.

## References

- [ 1 ] Nielsen M A , Chuang I L. Quantum Computation and Quantum Information. Beijing: Tsinghua University Press, 2015.
- [ 2 ] Bar-Gill N, Pham L M, Jarmola A, et al. Solid-state electronic spin coherence time approaching one second. *Nature Communications*, 2013, 4: Article number 1743.
- [ 3 ] Neumann P, Beck J, Steiner M, et al. Single-shot readout of a single nuclear spin. *Science*, 2010, 329(5991): 542–544.
- [ 4 ] Rong X, Geng J P, Wang Z X, et al. Implementation of dynamically corrected gates on a single electron spin in diamond. *Phys. Rev. Lett.*, 2014, 112: 050503.
- [ 5 ] Mamin H J, Kim M, Sherwood M H, et al. Nanoscale nuclear magnetic resonance with a nitrogen-vacancy spin sensor. *Science*, 2013, 339(6119): 557–560.
- [ 6 ] Said R S, Twamley J. Robust control of entanglement in a nitrogen-vacancy center coupled to a C13 nuclear spin in diamond. *Physical Review A*, 2009, 80(3): 032303.
- [ 7 ] Dolde F, Jakobi I, Naydenov B, et al. Room-temperature entanglement between single defect spins in diamond. *Nature Physics*, 2013, 9(3): 139–143.
- [ 8 ] Dolde F, Bergholm V, Wang Y, et al. High-fidelity spin entanglement using optimal control. *Nature Communications*, 2014, 5: Article number 3371.
- [ 9 ] Sekiguchi Y, Niikura N, Kuroiwa R, et al. Optical holonomic single quantum gates with a geometric spin under a zero field. *Nature Photonics*, 2017, 11: 309–314.
- [ 10 ] Humphreys P C, Kalb N, Morits J P J, et al. Deterministic delivery of remote entanglement on a quantum network. *Nature*, 2018, 558(7709): 268–273.
- [ 11 ] Beterov I I, Khamzina N G, Tret'yakov B D, et al. Resonant dipole-dipole interaction of Rydberg atoms for realisation of quantum computations. *Quantum Electronics*, 2018, 48(5): 453–459.
- [ 12 ] King B E. Demonstration of a fundamental quantum logic gate. *Phys. Rev. Lett.*, 1995, 75(25): 4714–4717.
- [ 13 ] Jaksch D, Cirac J I, Zoller P, et al. Fast quantum gates for neutral atoms. *Phys. Rev. Lett.*, 2000, 85(10): 2208–2211.
- [ 14 ] Lim J, Lee H G, Ahn J. Review of cold Rydberg atoms and their applications. *Journal of the Korean Physical Society*, 2013, 63(4): 867–876.
- [ 15 ] Goldman M L, Sipahigil A, Doherty M W, et al. Phonon-induced population dynamics and intersystem crossing in nitrogen-vacancy centers. *Phys. Rev. Lett.*, 2015, 114:

- 145502.
- [16] Hettich C. Coherent optical dipole coupling of two individual molecules at nanometre separation. Konstanz, Germany: University of Konstanz, 2002.
- [17] Varada G V, Agarwal G S. Two photon resonance induced by the dipole-dipole interaction. *Physical Review A*, 1992, 45(9): 6721–6729.
- [18] Doherty M W, Manson N B, Delaney P, et al. The nitrogen-vacancy colour centre in diamond. *Physics Reports*, 2013, 528(1): 1–45.
- [19] Lee K W, Lee D, Ovarthaiyapong P, et al. Strain coupling of a mechanical resonator to a single quantum emitter in diamond. *Phys. Rev. Applied*, 2016, 6: 034005.
- [20] Tamarat Ph, Gaebel T, Rabeau J R, et al. Stark shift control of single optical centers in diamond. *Phys. Rev. Lett.*, 2006, 97: 083002.
- [21] Xu Z J, Yin Z Q, Han Q K, et al. Quantum information processing with closely-spaced diamond color centers in strain and magnetic fields. *Optical Materials Express*, 2019, 9: 4654–4668.
- [22] Schirhagl R, Chang K, Loretz M, et al. Nitrogen-vacancy centers in diamond: Nanoscale sensors for physics and biology. *Annual Review of Physical Chemistry*, 2014, 65(1): 83–105.
- [23] Zablotskii V, Polyakova T, Dejneka A. Cells in the nonuniform magnetic world: How cells respond to high-gradient magnetic fields. *BioEssays*, 2018, 40(8): e1800017.
- [24] Batalov A, Zierl C, Gaebel T, et al. Temporal coherence of photons emitted by single nitrogen-vacancy defect centers in diamond using optical Rabi-oscillations. *Phys. Rev. Lett.*, 2008, 100(7): 077401.
- [25] Bienfait A, Pla J J, Kubo Y, et al. Controlling spin relaxation with a cavity. *Nature*, 2016, 531(7592): 74–77.
- [26] Goy P, Raimond J M, Gross M, et al. Observation of cavity-enhanced single-atom spontaneous emission. *Phys. Rev. Lett.*, 1983, 50(24): 1903–1906.
- [27] Hoang T H C, Durán-Valdeiglesias E, Alonso-Ramos C, et al. Narrow-linewidth carbon nanotube emission in silicon hollow-core photonic crystal cavity. *Optics Letters*, 2017, 42(11): 2228–2231.
- [28] Takiguchi M, Sumikura H, Birowosuto M D, et al. Enhanced and suppressed spontaneous emission from a buried heterostructure photonic crystal cavity. In: 2013 Conference on Lasers and Electro-Optics Pacific Rim. Washington DC: Optical Society of America, 2013.
- [29] Heinzen D J, Childs J J, Thomas J E, et al. Enhanced and inhibited visible spontaneous emission by atoms in a confocal resonator. *Phys. Rev. Lett.*, 1987, 58(13): 1320–1323.
- [30] Yamamoto Y, Machida S, Horikoshi Y, et al. Enhanced and inhibited spontaneous emission of free excitons in GaAs quantum wells in a microcavity. *Optics Communications*, 1991, 80: 337–342.
- [31] Stortebom J, Dolan P, Castelletto S, et al. Lifetime investigation of single nitrogen vacancy centres in nanodiamonds. *Optics Express*, 2015, 23(9): 11327–11333.
- [32] Scully M O, Suhail Zubairy M. *Quantum Optics*. Beijing: World Publishing, 2000.
- [33] Wilmott C, Wild P. A construction of a generalized quantum SWAP gate. <https://arxiv.org/abs/0811.1684v1>.
- [34] Toyli D M, Weis C D, Fuchs G D, et al. Chip-scale nanofabrication of single spins and spin arrays in diamond. *Nano Letters*, 2010, 10(8): 3168–3172.
- [35] Tamural S, Koike G, Komatsubara A, et al. Array of bright silicon-vacancy centers in diamond fabricated by low-energy focused ion beam implantation. *Applied Physics Express*, 2014, 7(11): 115201.
- [36] Scarabelli D, Trusheim M, Gaathon O, et al. Nanoscale engineering of closely-spaced electronic spins in diamond. *Nano Letters*, 2016, 16(8): 4982–4990.

## 金刚石 NV 色心间基于电偶极耦合的快速受控非门

史舜阳<sup>1,2,3,4</sup>, 季文韬<sup>1,2,3,4</sup>, 王亚<sup>1,2,3,4\*</sup>, 杜江峰<sup>1,2,3,4\*</sup>

1. 中国科学技术大学近代物理系, 安徽合肥 230026;

2. 合肥微尺度物质科学国家研究中心, 安徽合肥 230026;

3. 中国科学技术大学中科院微观磁共振实验室, 安徽合肥 230026;

4. 中国科学技术大学量子信息与量子物理协同创新中心, 安徽合肥 230026

\* 通讯作者. E-mail: ywustc@ustc.edu.cn; djf@ustc.edu.cn

**摘要:** 提出了一种在金刚石中两个临近氮-空位色心 (nitrogen-vacancy color center, 简称 NV 色心) 之间施加受控非门 (C-NOT gate) 的新方案. 在该方案中, 临近 NV 色心间的强电偶极耦合将导致态依赖的能级移动, 从而施加可控的激光共振激发可以实现快速受控相位门 (C-phase gate), 结合单比特操作, 可以快速实现 C-NOT 门. 在两个相邻 10 nm 的 NV 色心之间, C-NOT 门操作时间最快可达 120 ns, 比传统磁偶极方式快了 2 个量级. 为了降低激发态自发辐射的影响, 提出利用非共振腔抑制自发辐射. 模拟结果显示 C-phase 门操控保真度可以达到 98.88%. 最后, 将该方案扩展到一维 NV 色心自旋链.

**关键词:** 氮-空位色心; 量子计算; 受控非门; 一维自旋链